Hybrid zeolitic-mesostructured materials as supports of metallocene polymerization catalysts

A. Carrero [a,*], R. van Grieken [b], B. Paredes [b]

[a] Department of Chemical and Energy Technology, ESCET, Universidad Rey Juan Carlos, c/Tulipan s/n, 28933 Mostoles, Madrid, Spain
[b] Department of Chemical and Environmental Technology, ESCET, Universidad Rey Juan Carlos, c/Tulipan s/n, 28933 Mostoles, Madrid, Spain

ARTICLE INFO

ABSTRACT

The potential application of hybrid ZSM-5/Al-MCM-41 zeolitic-mesostructured materials as supports of metallocene polymerization catalysts has been investigated and compared with the behaviour of standard mesoporous Al-MCM-41 and microporous ZSM-5 samples. Hybrid zeolitic-mesostructured solids were prepared from zeolite seeds obtained with different Si/Al molar ratios (15, 30 and 60), which were assembled around cetyltrimethylammonium bromide (CTAB) micelles to obtain hybrid materials having a combination of both zeolitic and mesostructured features. $(nBuCp)_2ZrCl_2$/MAO catalytic system was impregnated onto the above mentioned solid supports and tested in ethylene polymerization at 70 °C and 5 bar of ethylene pressure. Supports and heterogeneous catalysts were characterized by X-ray powder diffraction, nitrogen adsorption–desorption isotherms at 77 K, transmission electron microscopy, ^{27}Al-MAS-NMR, ICP-atomic emission spectroscopy and UV–vis spectroscopy.

Catalysts supported over hybrid ZSM-5/Al-MCM-41 (Si/Al = 30–60) exhibited the best catalytic activity followed by those supported on Al-MCM-41 (Si/Al = 30–60). However, catalyst supported on ZSM-5 gave lower polymerization activity because of its microporous structure with narrower pores and lower textural properties than hybrid and mesoporous materials.

Although higher acid site population shown by hybrid materials could contribute to the stabilization of the metallocene system on the support, in this case their better catalytic performance is mainly ascribed to the larger textural properties.

© 2011 Elsevier B.V. All rights reserved.

1. Introduction

Polyolefins are the most widely used commodity thermoplastics, since few materials can match their excellent combination of good chemical and physical properties together with economy. Among polyolefins, polyethylene has a quite large usage because its chemical stability and great range of physical properties that make it suitable for a broad range of applications, from strong, flexible films and coatings to rigid containers [1].

The present stage of evolution in polyolefin industry is mainly due to the developments in the catalysis field. The discovery of metallocene with methylaluminoxane (MAO) catalytic systems allowed the synthesis of new polyolefins, with properties different from those obtained through the traditional Ziegler–Natta catalysts [2]. The main disadvantages of the homogeneous character of the original metallocene systems are the very large amount of methylaluminoxane (MAO) needed to achieve maximum metallocene catalytic activity and the lack of morphology control of the polymer particle, which leads to reactor fouling, with frequent stoppage for equipment cleaning. This leads to the impossibility of using metallocene directly in the existing slurry and gas-phase industrial plants [2–5]. Searching for a solution regarding this difficulty, supported metallocene catalysts have been deeply investigated in the last 20 years [6].

The type of the support as well as the technique used for supporting the metallocene and MAO has a crucial influence on the catalyst behaviour. According with the literature, several techniques for immobilizing metallocenes and MAO have been proposed [4,6]: (1) adsorption of MAO onto the support followed by addition of the metallocene; (2) immobilization of the metallocene on the support, followed by contact with MAO in the polymerization reactor; and (3) immobilization of the metallocene on the support, followed by treatment with MAO, producing a catalyst which does not require MAO during polymerization, but generally requires aluminium alkyls. In this last method it is also possible to put in contact MAO and metallocene in solution before supporting, which is supposed to maximize the number of active centres

* Corresponding author. Tel.: +34 91 488 70 88; fax: +34 91 488 70 68.
E-mail addresses: alicia.carrero@urjc.es (A. Carrero), rafael.vangrieken@urjc.es (R. van Grieken), beatriz.paredes@urjc.es (B. Paredes).

because of activating the metallocene in solution instead of carrying out the process with one or the other component in an immobilized state [4].

Regarding the supports for the immobilization, amorphous silica is definitely the most common one because it has high surface area and porosity, and is stable and inert under reaction and processing conditions. Other quite employed supports are alumina and magnesium dichloride [6]. The common characteristic of these inorganic carriers is a broad pore size distribution and an amorphous structure. Therefore, having into account that the pore shape, pore size, pore size distribution and pore connectivity are the most important factors for the adsorption reaction between the active component and the support, zeolites as well as mesoporous materials [7,8] have recently gained growing interest as supports for metallocene catalysis aiming to increase catalyst activity or to exhibit different polymer properties [4,6,10].

Previous studies have described the anchorage of metallocenes on zeolites [11–18] and mesoporous materials like MCM-41 and SBA-15 [19–25]. The results evidenced that textural properties of the ordered microporous and mesoporous supports influence the structure of the supported metallocenes and, therefore their catalytic activity. In this sense, supports with narrower pore diameters presented lower catalytic activities suggesting the higher probability of inactive bimolecular species formation due to the proximity among the catalytic precursors supported within micropores. Smaller pores also contribute to the formation of surface obstacles, which may hinder reactant diffusion [10,19]. These zeolite considerations make ordered mesoporous aluminosilicates more attractive for their application as metallocene supports, since they have larger pores (2–10 nm), which could enable metallocene and MAO molecules to be anchored not only on the surface but also inside the porous structure leading to polyethylene chains grow [9,20].

Besides, it has been pointed out by several authors the influence of solid supports acid properties on the activation of metallocene catalysts and, consequently on the corresponding polymerization activity [17,24,26–28]. It is generally accepted that the active species in the metallocene catalytic system for olefin polymerization is a coordinately unsaturated transition metal cation stabilized by bulky counter-anions such as the Lewis acidic methylaluminoxane. Therefore, it has been described in the literature how aluminium atoms contained in the support may stabilize and generate the active species in polymerization.

Zeolites are characterized by a large range of acidity from which to choose a support with adequate Lewis acidity, but as a solution to the pore size limitations described above, Al-MCM-41 has been widely investigated, with different Si/Al molar ratios, showing that its Lewis acidity play an important role for anchoring zirconocenes [21,22,29] in spite of its acid strength is considerably weaker as compared with that of zeolite [30] although aluminium could be easily incorporated into the MCM-41 framework. However, supported metallocenes are still less active compared with homogenous systems and this problem needs to be overcome when using heterogeneous catalysts. For this reason, the development of new support/catalyst/cocatalyst combinations remains a fruitful field of research.

Based on the above mentioned considerations, in the present work hybrid zeolitic-mesoporous materials synthesized from ZSM-5 seeds, prepared with Si/Al molar ratios of 15, 30 and 60, are investigated as supports for the catalytic system $(nBuCp)_2ZrCl_2$/MAO. These hybrid materials present a mesostructured ordering similar to that of Al-MCM-41, with the difference that the walls are not amorphous but they consist of zeolitic units [31,32]. For comparative purposes $(nBuCp)_2ZrCl_2$/MAO was also supported on conventional ZSM-5 and Al-MCM-41 materials and tested in ethylene polymerization.

2. Materials and methods

2.1. Supports synthesis and catalysts preparation

Hybrid zeolitic-mesoporous materials were synthesized from zeolite seeds, obtained in the early stages of ZSM-5 crystallization, assembled around cetyltrimethylammonium bromide (CTAB) micelles. Thereby, in the first step a ZSM-5 synthesis gel was prepared according to a procedure earlier reported [33]. The gel was aged for 40 h at room temperature in order to promote the generation of the zeolite seeds. Thereafter, the formation of the mesostructure was achieved by the addition of the surfactant (CTAB, Aldrich) and water to the prepared seed solution. After an additional aging period of 5 h at room temperature, the mixture was transferred into an autoclave and heated at 110 °C for 2 days under static conditions. The solid material so obtained was recovered by filtration, being denoted as MCM-ZSM-x, where x represents the Si/Al molar ratio in the synthesis (15, 30 and 60). Finally, the MCM-ZSM samples were subjected to a calcination treatment at 550 °C to remove the occluded organics.
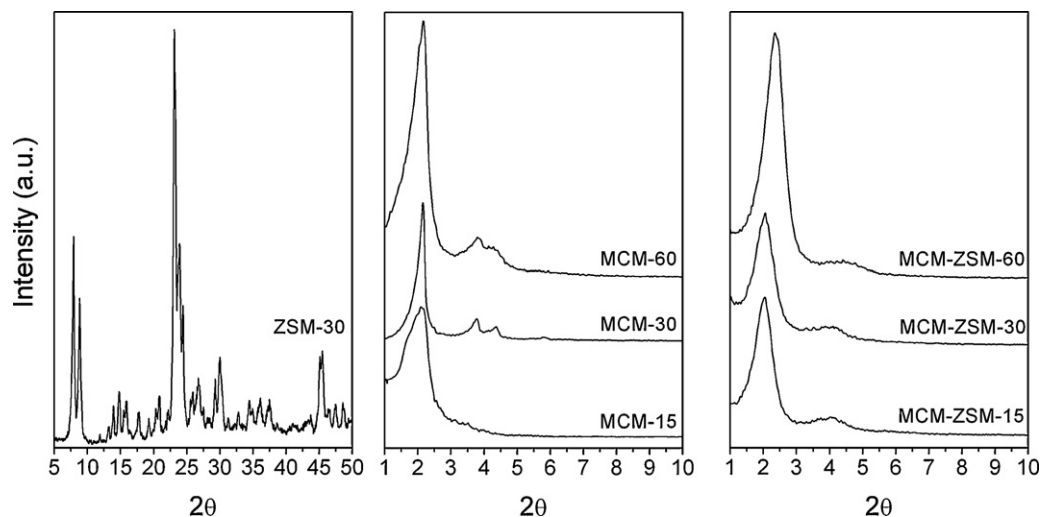

Fig. 1. X-ray diffraction patterns of the synthesized support materials.

Besides, standard Al-MCM-41 were synthesized according with the procedure previously described [34], being designated as MCM-*x*, where *x* represents the Si/Al molar ratio in the synthesis gel (15, 30 and 60). Likewise, nanocrystalline ZSM-5 zeolite with a Si/Al molar ratio of 30 (ZSM-30) was synthesized according to the literature [33].

MAO/metallocene grafting experiments were performed under inert nitrogen atmosphere using the Schlenk technique and glove box. All the synthesized materials were used as supports of the catalytic system. The metallocene, bis(n-butylcyclopentadienyl)zirconium dichloride ((nBuCp)$_2$ZrCl$_2$, 97 wt%, Aldrich), was dissolved at room temperature in a solution of methylaluminoxane (MAO, 10 wt% in toluene, Aldrich) and dry toluene (99 wt%, Scharlab). The amounts of MAO and metallocene were calculated in order to get supported catalysts with 0.25 wt% of zirconium and 14 wt% of aluminium from MAO which corresponds to an Al$_{MAO}$/Zr molar ratio of 190, according to previous studies [35]. This solution was added to the support material ($V_{solution}/V_{pores} \sim 3$) in order to get a homogeneous slurry [4], and after a time reaction of 3 h under nitrogen flow at room temperature, the solid was collected and stored in glove box.

2.2. Characterization of supports and catalysts

Nitrogen adsorption–desorption isotherms at 77 K were obtained on a Micromeritics TRISTAR 2050 sorptometer. Prior to the adsorption, the samples were outgassed under vacuum at 300 °C for 2 h. Surface areas were calculated according to the BET method. The determination of the pore size distribution was done by applying the BJH model with the DFT Plus Programme (Micromeritics) to the adsorption branch of the isotherm. Pore volumes were determined from the nitrogen adsorbed volume at $P/P_0 = 0.98$.

The NH$_3$-TPD measurements were carried out in a Micromeritics 2910 (TPD/TPR) equipment with a thermal conductivity detector (TCD). Prior to the measurements, about 100 mg of the sample were flushed with helium (50 cm^3 min^{-1}) at 550 °C. After cooling at 180 °C, ammonia adsorption was carried out during 30 min with an ammonia flow rate of 35 cm^3 min^{-1}. Physically adsorbed ammonia was removed by purging with helium (50 cm^3 min^{-1}) for 90 min, before the NH$_3$-TPD measurement. The NH$_3$-TPD of the samples was carried out by increasing the temperature linearly from 150 to 550 °C with a heating rate of 15 °C min^{-1} holding for 30 min and helium flow rate of 35 cm^3 min^{-1}.

Solid-state ^{27}Al-MAS-NMR experiments were performed on a Varian-Infinity 400 MHz spectrometer fitted with a 9.4 T magnetic field. ^{27}Al nucleus resonates at a frequency of 104.16 MHz. For ^{27}Al acquisition spinning rate, pulse, number of scans and repetition delay were, 12 kHz, π/2, 4000 scans and 1.5 s, respectively.

X-ray powder diffraction (XRD) spectra were taken in a Phillips X'PERT MPD diffractometer with Cu Kα radiation. Transmission electron micrographs (TEM) and was taken on a Phillips TECNAI 20 microscope equipped with a LaB6 filament and an accelerating voltage of 200 kV. Scanning electron micrographs (SEM) were taken on a Phillips XL30 ESEM (Environmental Scanning Electron Microscope) equipped with a tungsten filament and an accelerating voltage of 15 kV. The Si/Al atomic ratios of the supports as well as Al$_{MAO}$/Zr molar ratio of the supported catalysts were determined by ICP-AES on a Varian Vista AX Axial CCD Simultaneous ICP-AES spectrophotometer.

UV–vis spectroscopic studies of supported catalysts were performed. The catalyst samples were sealed into 1 cm quartz cells with Teflon stoppers. The UV–vis spectra were scanned using a Varian Cary 500 spectrophotometer. An integrating sphere diffuse reflectance accessory was used to enable the measurement in reflectance mode. A high scanning speed was used, 450 nm min^{-1}, to allow fast measurement, in wavelength range 200–600 nm.

2.3. Ethylene polymerization and polymer characterization

Ethylene polymerizations were performed at 70 °C in a 2.0-L stirred-glass reactor filled with 1.0-L of n-heptane (99%, Scharlab) as diluent, and tri-isobutylamunimum (TIBA, 30 wt% in heptane, Witco) as scavenger. Ethylene (99.99%, Air Liquide) was deoxygenated and dried through columns containing R-3/15 BASF catalyst, alumina and 3 Å molecular sieves. The flow rate needed to keep a constant pressure of 5 bars during the polymerization was measured with a mass-flow indicator (Bronkhorst Hi-Tec). After
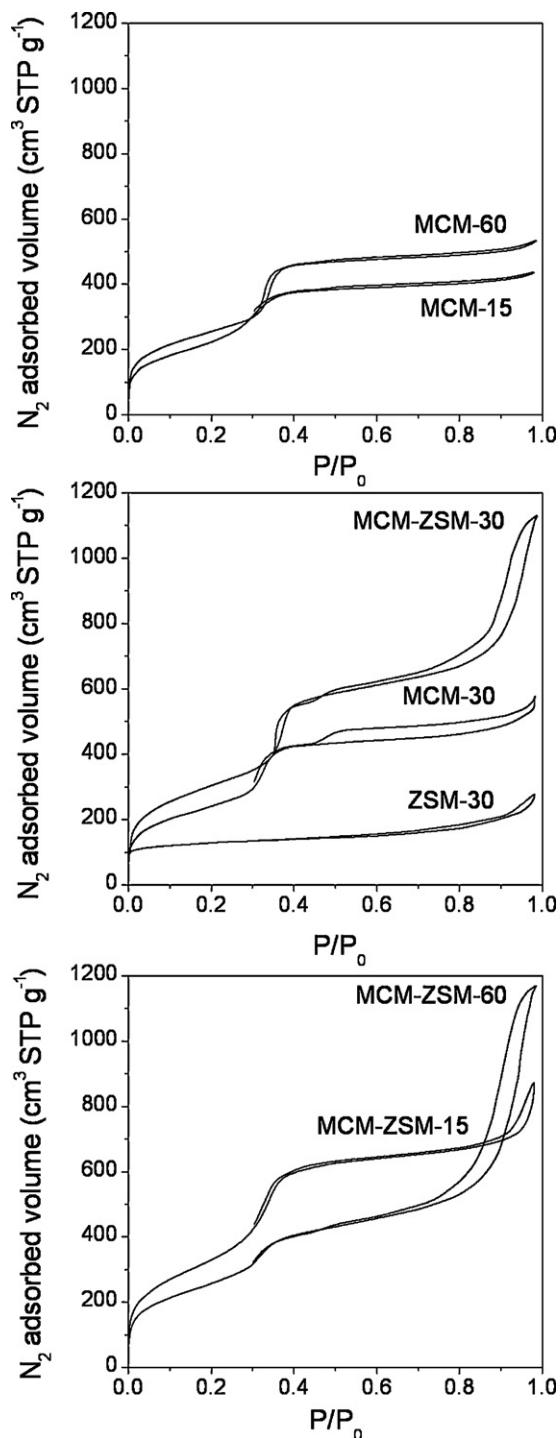

Fig. 2. N$_2$ adsorption–desorption isotherms at 77 K of the synthesized support materials.

Table 1
Physicochemical properties of the synthesized materials.

Support	Si/Al solid[a]	A_{BET} (m^2 g^{-1})	V_{pore} (cm^3 g^{-1})	D_{pore} (Å)	Acid sites (mequiv. NH$_3$/g)[b]	T_{peak} (°C)[b]	Al$_{tetra}$ (%)[c]
ZSM-30	24.4	448	0.174	5.5	0.37	412	96.9
MCM-60	50.3	926	0.813	25.6	0.07	–	47.6
MCM-30	27.1	874	0.828	24.4	0.19	258	55.9
MCM-15	12.6	812	0.665	22.9	0.28	263	26.8
MCM-ZSM-60	47.0	1109	1.451	25.3	0.17	308	89.9
MCM-ZSM-30	23.9	1096	1.426	27.9	0.22	302	58.4
MCM-ZSM-15	12.0	934	1.259	24.0	0.33	306	22.1

[a] Molar ratio determined by ICP-AES analysis.
[b] Determined from NH$_3$-TPD analysis.
[c] Determined from ^{27}Al-MAS-NMR analysis.

30 min, the polymerization was stopped by depressurization and polyethylene was recovered, filtered and dried for 12 h at 70 °C.

Molecular weight distributions of polymers obtained with metallocene catalysts were determined with a Waters ALLIANCE GPCV 2000 gel permeation chromatograph (GPC). This apparatus is equipped with a refractometer, a viscosimeter and three Styragel HT type columns (HT3, HT4 and HT6) with exclusion limits of 1×10^7 for polystyrene. 1,2,4-Trichlorobenzene was used as solvent, at a flow rate of 1 cm^3 min^{-1}. The analyses were performed at 145 °C. The columns were calibrated with narrow molar mass distribution polystyrene and with linear low density polyethylenes standards. Polymer melting points (T_m) and crystallinities were determined in a METTLER TOLEDO DSC822 differential scanning calorimeter (DSC), using a heating rate of 10 °C min^{-1} in the temperature range 23–160 °C. The heating cycle was performed twice, but only the results of the second scan were reported, because the former could be influenced by the mechanical and thermal history of the samples. In order to analyze the morphology of the polyethylene obtained, scanning electron microscopy (SEM) was used by means of a Phillips XL30 ESEM (Environmental Scanning Electron Microscope) equipped with a tungsten filament and an accelerating voltage of 15 kV.

3. Results and discussion

3.1. Supports characterization

Fig. 1 compares the XRD patterns of synthesized support materials. The wide-angle spectra of ZSM-30 exhibit the XRD pattern typical of the MFI structure [33]. Al-MCM-41 type materials show a main broad diffraction peak, placed at $2\theta = 2.0$–$2.2°$, which is associated to the (1 0 0) plane and assigned to the presence of a hexagonal mesopore array also observed in MCM-ZSM hybrid samples [30]. Two other peaks at bigger angles can be distinguished for MCM-60 and MCM-30, indexed as (1 1 0) and (2 0 0), suggesting less ordered structures in MCM-15 as well as hybrid materials. The XRD patterns of hybrid materials taken at high angles did not present zeolitic peaks, which indicate that the X-ray zeolitic crystallinity is absent, at least at a macroscopic level, confirming the synthesis of an hybrid material without phase segregation [31].

Fig. 2 illustrates the N$_2$ adsorption–desorption isotherms at 77 K. Al-MCM-41 materials present a type IV adsorption isotherms (according to the IUPAC classification) with the typical shape for mesoporous materials. The MCM-ZSM hybrid samples exhibit a great N$_2$ adsorption at high relative pressures, which denotes the presence of a large amount of interparticle porosity. On the contrary, ZSM-30 zeolite exhibits the isotherm characteristic of MFI microporous structure [33].

Table 1 summarized physicochemical properties of synthesized solid supports. As it can be observed, Si/Al ratios determined by chemical analysis were close to those in the synthesis gel, more markedly for MCM materials than for MCM-ZSM. Regarding textural properties, microporous ZSM-30 zeolite has lower surface area, pore volume and pore size than mesoporous materials. It is noticeable that MCM-ZSM hybrid materials have quite higher pore volumes than MCM materials and a microporosity related with the presence of zeolite micropores, that is, the results of the N$_2$ adsorption measurements confirm that the MCM-ZSM hybrid samples posses textural properties that combine those of zeolites and ordered mesoporous materials [31]. In general, for both type of mesostructured materials, MCM and MCM-ZSM, a slight decrease
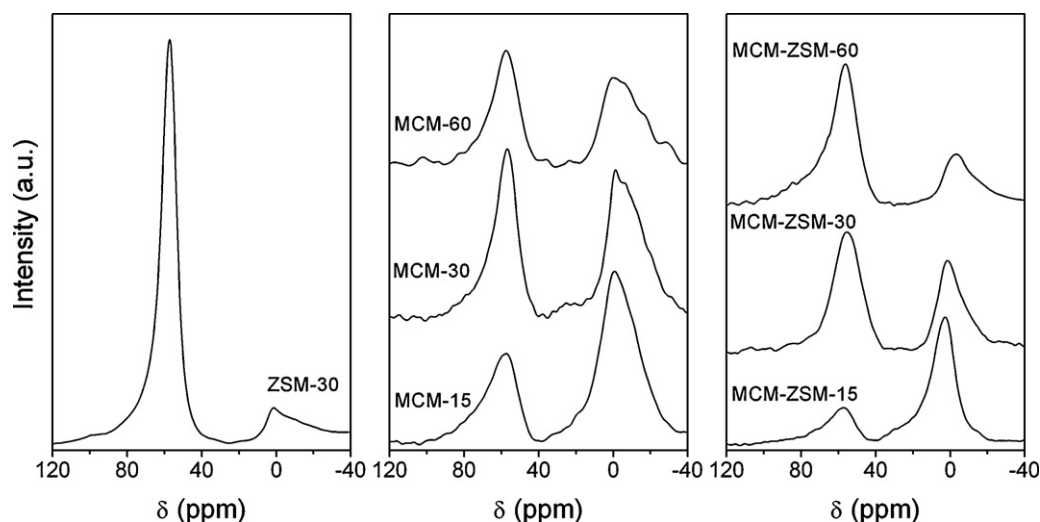

Fig. 3. ^{27}Al-MAS-NMR spectra of the synthesized support materials.

in textural properties is observed as the Si/Al molar ratio does, suggesting a change in the pore structure of these materials at low Si/Al molar ratio, that is, a lower ordered structure. Acid properties measured by ammonia TPD experiments are also included in Table 1. The amount of ammonia desorbed and the temperature at which that desorption takes place are clearly lower for both the hybrid and the Al-MCM-41 materials in regards to that of ZSM-30 zeolite synthesized in the protonic form. The presence of zeolitic units in the pore walls of hybrid materials results in acidic properties intermediate between the zeolite and ordered mesoporous materials, that is, more and stronger acid sites found in hybrid materials in comparison with Al-MCM-41 at Si/Al molar ratios in the range 60–15. Likewise, the amount of ammonia desorbed from the samples is lower as the Si/Al molar ratio increases.

[27] Al-MAS-NMR spectra are shown in Fig. 3. ZSM-30 zeolite presents a main peak placed at 57 ppm corresponding to tetrahedrally co-ordinated aluminium along with a smaller one at ~0 ppm related to octahedrally co-ordinated aluminium. From the area corresponding to these peaks it is possible to get an estimation of the relative contribution of both tetrahedral and octahedral aluminium species in each sample (see last column in Table 1, in which the percentage corresponding to tetrahedrally co-ordinated aluminium is summarized). Aluminium in ZSM-30 zeolite is mostly tetrahedrally co-ordinated while Al-MCM-41 mesoporous materials present an important fraction of octahedral Al atoms, mainly at Si/Al molar ratios of 15, which is in agreement with the lower stability of ordered mesoporous materials compared to zeolites, as indicated by numerous authors in the previous literature, due to the amorphous nature of their pore walls. On line with previous explanations, the presence of zeolitic units in the pore walls of hybrid materials increases the contribution of tetrahedral aluminium mainly at high Si/Al molar ratios as 60, which indicates the bigger stability of the Al atoms in the former, that contribution decreases as the Si/Al molar ratio increases [34].

Fig. 4 illustrates TEM images of solids supports. The ZSM-30 sample (Fig. 4 (a)) is formed by ~20 nm sized nanocrystals forming aggregates, while Fig. 4(b) depicts the hexagonal arrangement of MCM-30 mesoporous channels, which become less organized for MCM-ZSM-30 (Fig. 4(c)), in agreement with XRD (Fig. 1), which exhibits a complete uniform wormhole motif.

3.2. Catalysts characterization, polymerization activity and polyethylene properties

Metallocene activation has been extensively studied by UV–vis spectroscopy since the spectrum of zirconocene dichloride consists of at least one broad ligand to metal charge transfer (LMCT) absorption band, this LMCT band is a rather sensitive indicator of changes in the frontier orbital energies. With metallocene ionization the electron density at a Zr atom decreases markedly, thus there is a lower LMCT energy [36,37].

Fig. 5 presents the spectra of $(nBuCp)_2ZrCl_2$/MAO supported over ZSM-30, MCM-30 and MCM-ZSM-30. Since zirconocene was allowed to react with MAO prior to addition onto the supports, the intense band observed at 263 nm with a shoulder at 270 nm, may be related with the interactions between the support and methylaluminoxane molecules non reacted with $(nBuCp)_2ZrCl_2$ metallocene catalyst [37]. The broad band placed around 350 nm in CAT-ZSM-30 spectra suggests the presence of the catalyst precursor mono- and/or dimethylated. This band appears shifted to higher wavelenghts in the spectrum corresponding to catalysts supported over MCM-30 and MCM-ZSM-30 carriers. Besides, the formation of Zr cationic species should lead to LMCT bathochromic shift observed in MCM-ZSM hybrid samples as a shoulder around 400 nm.

The leaving group abstraction or ionization mechanism can be understood as an acid-base reaction in which the metallocene is
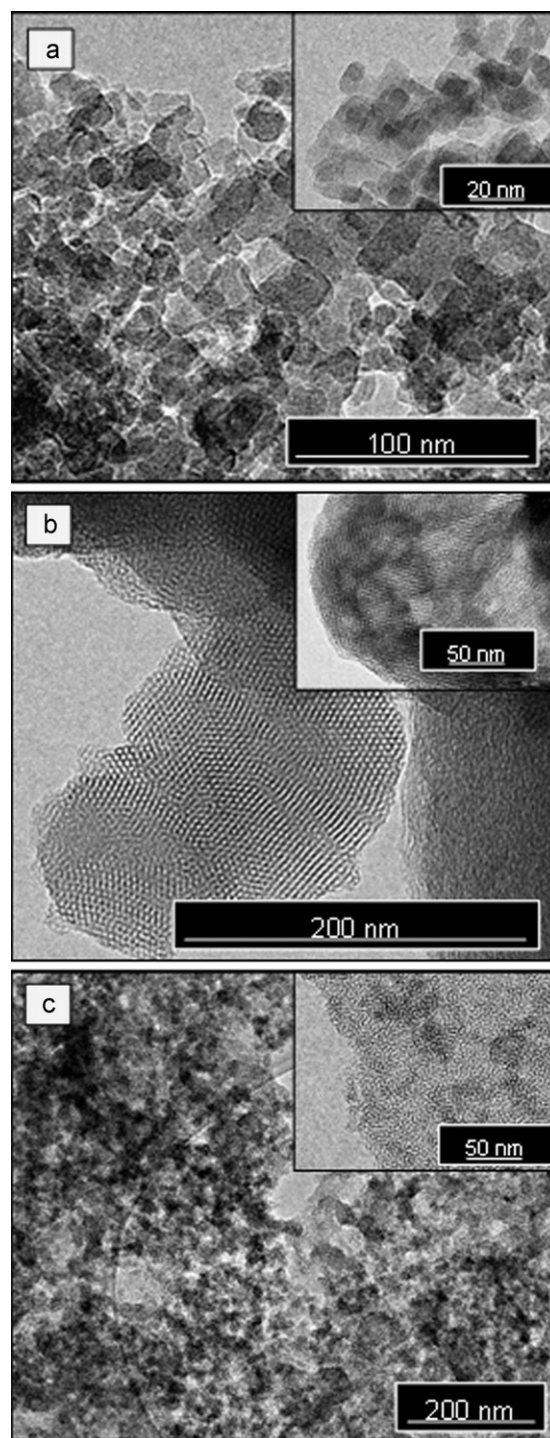

Fig. 4. Transmission electron microscopy images of the synthesized materials (a) ZSM5-30, (b) MCM-30 and (c) MCM-ZSM-30.

the base, thus the acid site density and strength of the activator are important properties. It seems that the support material (zeolite, mesostructured or hybrid zeolitic-mesostructured) induces changes in the zirconocene activation as they are solid acids, affecting the frontier orbital energies. The contribution of the LMCT band seems to correlate with the acidity of the support. This fact is also confirmed by analyzing the UV–vis spectra of the metallocene system supported over hybrid materials (Fig. 5) with decreasing Si/Al molar ratios (increasing acidity), for which great contributions of the LMCT band are observed.

Table 2
Al_{MAO}/Zr molar ratio, ethylene polymerization activity and polyethylene properties of $(nBuCp)_2ZrCl_2/MAO$ supported catalysts.

Catalyst	(Al/Zr)[a] molar ratio	Activity (kg PE/mol Zr h bar)[b]	M_w (g/mol)[c]	M_w/M_n[c]	T_m (°C)[d]	α (%)[d]
CAT-ZSM-30	190	3040	296,432	2.18	137	57
CAT-MCM-60	187	8510	267,458	2.19	136	56
CAT-MCM-30	192	8320	213,255	2.08	136	56
CAT-MCM-15	192	6600	308,777	2.09	138	58
CAT-MCM-ZSM-60	197	11500	225,838	2.17	136	56
CAT-MCM-ZSM-30	199	11600	207,189	2.17	135	57
CAT-MCM-ZSM-15	195	8000	205,302	2.21	135	57

[a] Molar ratio determined by ICP-AES analysis.
[b] Polymerization conditions: catalyst: 50 mg; 1.0-L n-heptane; ethylene pressure: 5 bar; temperature: 70 °C; time: 30 min; TIBA was used as scavenger (Al_{TIBA}/Zr) = 800.
[c] Determined from GPC analysis.
[d] Determined from the second scan in DSC analysis.

The ethylene polymerization results are presented in Table 2. Considering supports materials synthesized with a Si/Al molar ratio of 30, the order in activity is as follows: CAT-ZSM-30 < CAT-MCM-30 < CAT-MCM-ZSM-30. These suggest that in this case polymerization activity is not related with support acid properties, so there are another properties influencing catalytic activity. The lowest activity found for the catalyst over ZSM-30 zeolite is in agreement with previous results [16,19]. Taking also into account MAO size [38], the low activity may be attributed to the extremely low pore size and volume of zeolites, which rule them out as polymerization catalysts supports [36]. The low pore volume imparts high strength to the zeolite matrix, which then cannot be fractured during polymerization in the usual way needed to generate activity. The low pore size makes very unlikely that the metallocene catalytic system might pass across the channels to be immobilized within the cavities being probable that the catalytic system is grafted on the borders of the pores and on the external surface of the support. This could guarantee easy access of monomer to the active sites. Nevertheless, such catalyst species are more exposed and more prone to catalyst deactivation [16,19].

Catalysts supported over hybrid materials lead to higher polymerization activities than over mesostructured type Al-MCM-41 materials. In this sense, support acid and textural properties are more or less responsible of the observed results. Comparing Tables 1 and 2 it can be deduced that increasing Al content (lower Si/Al ratio) MCM-41 and hybrid supports have more acid sites but polymerization activity does not increase. So, not all aluminium may be accessible for the stabilization of MAO/metallocene catalytic system [35,36]. It is known that support acid sites (Bronsted and/or Lewis) can influence on metallocene anchorage
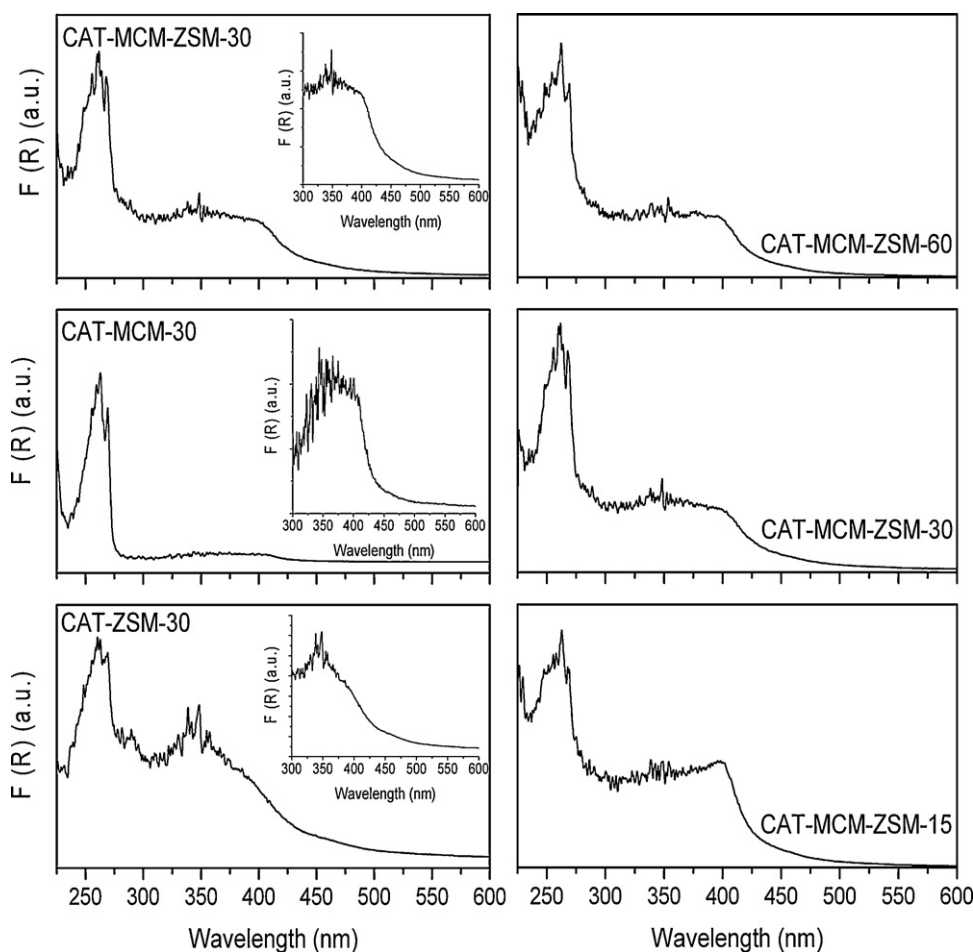
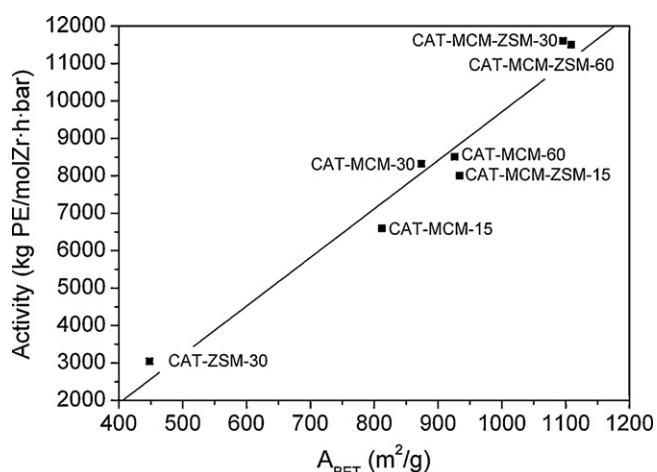**Fig. 5.** UV–vis spectra of $(nBuCp)_2ZrCl_2/MAO$ supported catalysts.

Fig. 6. Area BET of the $(nBuCp)_2ZrCl_2$/MAO support influence over the ethylene polymerization activity.

[21,22,28,29], however, we did not impregnate the metallocene directly on the support surface, we impregnate MAO and metallocene together. Since MAO amounts are larger than metallocene (Al_{MAO}/Zr molar ratio of 190), the support surface is mainly covered with the excess of MAO and after with metalloene. So, in this case support acid sites play a less important role than when metallocene is directly impregnated on the support without MAO.

Apart from acidic properties of the carriers, it is important to underline that the pore volume of hybrid materials is almost twice than those of mesostructured carriers, which could definitively influence their catalytic performance. Moreover, a correlation between catalytic activity and BET surface area has been found and it is shown in Fig. 6. Both textural parameters can contribute to a better dispersion of the catalytic system with lesser interaction between active sites avoiding bimolecular deactivation. Therefore, as also found in a previous work [24], support textural properties are more decisive in catalytic performance than their acid character.

Table 2 also summarizes polyethylene properties. All catalysts produced linear high-density polyethylene, with crystallinity values around 56–58%. The polymer MWD is very narrow, with
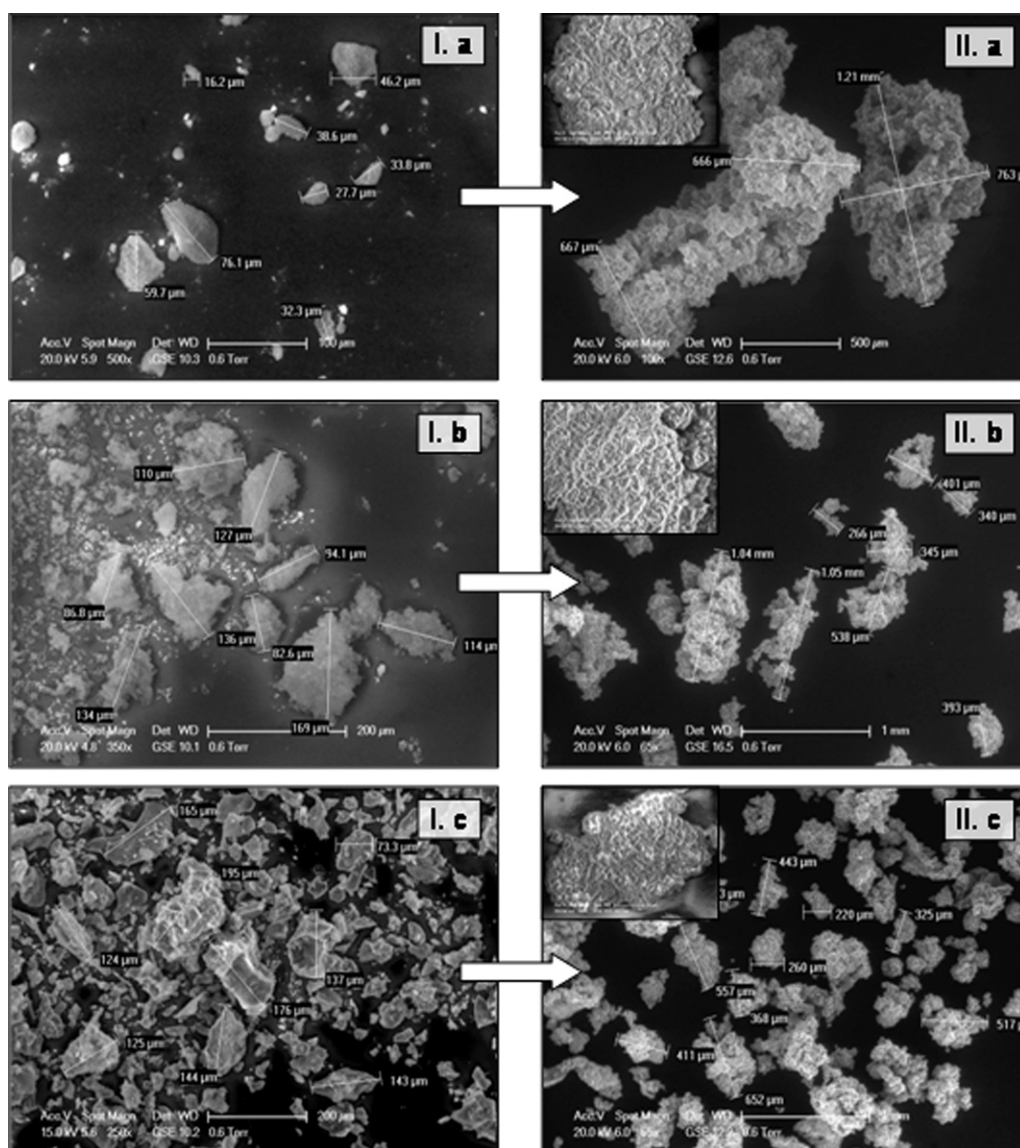

Fig. 7. Scanning electron microscopy images of the catalytic support (I) and the polyethylene (II) produced with $(nBuCp)_2ZrCl_2$/MAO supported over (a) ZSM, (b) MCM-30 and (c) MCM-ZSM-30.

dispersity index (M_w/M_n) approaching 2.0. This is the typical "single-site" distribution, and it indicates that the heterogeneity of the oxide surface does not exert a major influence on the active sites. In other words, the oxide surface does not seem to be part of the inner coordination sphere of the zirconium. Likewise, when the metallocene is activated by vastly different solid acid or MAO activators, little or no difference is observed in the molecular weight of the polymer produced. This behaviour is in contrast to many other oxide-supported catalysts, where the heterogeneity of the oxide surface is indeed reflected in a broad MWD [6].

In order to check the polymer morphology, SEM micrographs of PE samples were taken and showed in Fig. 7 in comparison with those of the corresponding carriers. Fragmentation and replica phenomena have been taken place since PE particles are made up of small polymer globules; these observed globules represent the growing polyethylene particles containing the primary catalyst particles with were exposed from the inside of the supported catalyst because of fragmentation processes [39]. These SEM investigations show how the polymer, which is formed in the pores of the support, is able to use its hydraulic forces and mechanically break up the structure of the support, thereby setting free new active centres. Extensive fragmentation and uniform particle growth are key features in the replication process and are dependent on a high surface area, a homogeneous distribution of catalytically active centres through the particle, and free access of the monomer to the innermost zones of the particle [6]. In this sense it is important to underline that polymer obtained with the catalytic system supported over the zeolite (CAT-ZSM-30) has grown 20 times, while using MCM-30 and MCM-ZSM-30 as supports the polyethylene growth has been 4.2 and 2.9 respectively. This fact points out that the polymer growth in CAT-ZSM-30 starts at and near the particle surface, leading to the formation of a shell of polyethylene around the catalyst particle, due to the above mentioned probable grafting of the catalytic system on the borders of the pores and on the external surface of the zeolite. Polymerization then takes place layer by layer, as the monomer gradually diffuses through the outer layers to the core, resulting in an onion-type internal morphology that leads to such big particles although the catalytic activity is the lowest.

4. Conclusions

Hybrid ZSM-5/Al-MCM-41 materials have demonstrated to be very suitable supports for $(nBuCp)_2ZrCl_2$/MAO catalytic system, showing better performance in ethylene polymerization than standard mesoporous Al-MCM-41 and microporous ZSM-5 samples. These hybrid materials present a mesostructured ordering similar to that of Al-MCM-41 with a type IV adsorption isotherm but with larger N_2 adsorption at high relative pressures that leads to quite higher pore volumes and BET surface areas than Al-MCM-41. The presence of zeolitic units in the pore walls of hybrid supports results in higher amounts of tetrahedral coordinated aluminium and intermediate acidic properties between ZSM-5 zeolite and Al-MCM-41 mesoporous materials.

UV–vis spectra of supported catalysts reveals that the nature of the solid support (zeolite, mesostructured or hybrid zeolitic-mesostructured) induces changes in the zirconocene activation as they are solid acids, affecting the frontier orbital energies that results in changes in the position and mainly in the contribution of the LMCT band. The lowest activity was reached with ZSM-5 zeolite as carrier, because of its microporous structure with low pore size and volume, being probable that the catalytic system was grafted on the borders of the pores and on the external surface. This fact was confirmed by SEM analyses of the polyethylene so obtained that reveals a layer by layer polymerization. Hybrid zeolitic-mesostructured materials provide metallocene supported

catalysts more active than mesostructured Al-MCM-41. Although hybrid materials have enhanced acid properties in comparison with Al-MCM-41, which can contribute to the stabilization of the metallocene system on the support, in this case their better catalytic performance is mainly related with larger textural properties leading to a better dispersion of the catalytic system with lesser interaction between active sites avoiding bimolecular deactivation.

All catalysts produced linear high-density polyethylene, with crystallinity values around 56–58% and very narrow molecular weight distribution.

References

[1] A.J. Peacock, Handbook of Polyethylene. Structures, Properties and Applications, Marcel Dekker Inc, New York, 2000.
[2] J.B.P. Soares, A.E. Hamielec, Polym. React. Eng. 3 (2) (1995) 131–200.
[3] M.R. Ribeiro, A. Deffieux, M.F. Portela, Ind. Eng. Chem. Res 36 (4) (1997) 1224–1237.
[4] G.G. Hlatky, Coord. Chem. Rev. 199 (2000) 235–329.
[5] G. Fink, B. Steinmetz, J. Zechlin, C. Przybyla, B. Tesche, Chem. Rev. 100 (4) (2000) 1377–1390.
[6] J.R. Severn, J.C. Chadwick, R. Duchateau, N. Friederichs, Chem. Rev. 105 (2005) 4073–4147.
[7] J. Cejka, S. Mintova, Catal. Rev. 49 (4) (2007) 457–509.
[8] J. Perez-Ramirez, C.H. Christensen, K. Egeblad, C.H. Christensen, J.C. Groen, Chem. Soc. Rev. 37 (11) (2008) 2530–2542.
[9] D. Trong On, D. Desplantier-Giscard, C. Danumah, S. Kaliaguine, Appl. Catal. A 222 (1–2) (2001) 299–357.
[10] F. Silveira, M.C. Martins, F.C. Stedile, S.B. Pergher, J.H.Z. dos Santos, J. Mol. Catal. A: Chem. 315 (2010) 213–220.
[11] M. Michelotti, A. Altomare, F. Ciardelli, E. Roland, J. Mol. Catal. A: Chem. 129 (2–3) (1998) 241–248.
[12] M. Michelotti, G. Arribas, S. Bronco, A. Altomare, J. Mol. Catal. A: Chem. 152 (1–2) (2000) 167–177.
[13] M.F.V. Marques, C.A. Henriques, J.L.F. Monteiro, S.M.C. Menezes, F.M.B. Coutinho, Macromol. Chem. Phys. 198 (1997) 3709–3717.
[14] S.C. Moreira, M.F.V. Marques, Eur. Polym. J. 37 (2001) 2123–2130.
[15] M.F.V. Marques, A.B. Marinha, J. Polym. Sci. A: Polym. Chem. 42 (12) (2004) 3038–3048.
[16] I.N. Meshkova, T.M. Ushakova, T.A. Ladygina, N.Yu Kovaleva, L.A. Novokshonova, Polym. Bull. 44 (2000) 461–468.
[17] V.I. Costa Vaya, P.G. Belelli, J.H.Z. dos Santos, M.L. Ferreira, D.E. Damiani, J. Mol. Catal. 204 (1) (2001) 1–10.
[18] M.F.V. Marques, S.C. Moreira, J. Mol. Catal. A: Chem. 192 (1–2) (2003) 93–101.
[19] F. Silveira, C.F. Petry, D. Pozebon, S.B. Pergher, C. Detoni, F.C. Stedile, J.H.Z. dos Santos, Appl. Catal. A 333 (1) (2007) 96–106.
[20] M.F.V. Marques, O.F.C. da Silva, A.C.S.L.S. Coutinho, A.S. de Araujo, Polym. Bull. 61 (2008) 415–423.
[21] H. Rahiala, I. Beurroies, T. Eklund, K. Hakala, R. Gougeon, P. Trens, J.B. Rosenholm, J. Catal. 188 (1) (1999) 14–23.
[22] K.-S. Lee, C.-G. Oh, J.-H. Yim, S.-K. Ihm, J. Mol. Catal. A: Chem. 159 (2) (2000) 301–308.
[23] D.E.B. Lopes, M. de Fatima, M.L. Dias, M. do Rosario, J.P. Lourenco, Eur. Polym. J. 40 (11) (2004) 2555–2563.
[24] A. Carrero, R. van Grieken, I. Suarez, B. Paredes, Polym. Eng. Sci. 48 (3) (2008) 606–616.
[25] C. Covarrubias, R. Quijada, Catal. Commun. 10 (2009) 995–1001.
[26] M. Jezequel, V. Dufaud, M.J. Ruiz-Garcia, F. Carrillo-Hermosilla, U. Neugebauer, G.P. Niccolai, F. Lefebvre, F. Bayard, J. Corker, S. Fiddy, J. Evans, J.P. Broyer, J. Malinge, J.M. Basset, J. Am. Chem. Soc. 123 (15) (2001) 3520–3540.
[27] J.M. Campos, J.P. Lourenco, A. Fernandes, M.R. Ribeiro, Catal. Commun. 10 (2008) 71–73.
[28] J.M. Campos, J.P. Lourenco, A. Fernandes, A.M. Rego, M.R. Ribeiro, J. Mol. Catal. A: Chem. 310 (2009) 1–8.
[29] T. Sano, Y. Oumi, Catal. Surv. Asia 8 (4) (2004) 295–304.
[30] C.T. Kresge, M.E. Leonowicz, W.J. Roth, J.C. Vartuli, J.S. Beck, Nature 359 (1992) 710–712.
[31] R.A. Garcia, D.P. Serrano, D. Otero, J. Anal. Appl. Pyrol. 74 (2005) 379–386.
[32] D.P. Serrano, R.A. Garcia, D. Otero, Appl. Catal. A 359 (2009) 69–78.
[33] R. van Grieken, J.L. Sotelo, J.M. Menendez, J.A. Melero, Microporous Mesoporous Mater. 39 (2000) 135–147.
[34] A. Matsumoto, H. Chen, K. Tsutsumi, M. Grün, K. Unger, Microporous Mesoporous Mater. 32 (1–2) (1999) 55–62.
[35] A. Carrero, R. van Grieken, B. Paredes, J. Appl. Polym. Sci. 120 (2011) 599–606.
[36] J.R. Severn, J.C. Chadwick, Tailor-made Polymers via Immobilization of Alpha-olefin Polymerization Catalysts, Wiley-VCH Verlag GmbH & Co. KGaA, Weinheim, 2008.
[37] N.I. Maekelae-Vaarne, K. Kallio, K.-H. Reichert, M.A. Leskelae, Macromol. Chem. Phys. 204 (8) (2003) 1085–1089.
[38] D.E. Babushkin, H.H. Brintzinger, J. Am. Chem. Soc. 124 (43) (2002) 12869–12873.
[39] C.-H. Lin, C.-Y. Sheu, Macromol. Rapid Commun. 21 (15) (2000) 1058–1062.